

# Non-localized cluster dynamics and nuclear molecular structure

H. Horiuchi

RCNP, Osaka Univ., Osaka  
and IAS, Kyoto

1. Introduction
2. Hybrid-Brink-THSR wave function
3. RGM/GCM w.f.  $\approx$  single THSR w.f.
4.  $(\text{ProlateTHSR})_J \approx (\text{OblateTHSR})_J \approx (\text{SphericalTHSR})_J$
5. Physical oblate deformation does not exist in  $^{16}\text{O} + \alpha$  THSR and the reason of it
6. Container picture for cluster structure and effectively-localized clustering
7. Summarizing discussions

RCNP Workshop on Clustering Phenomena in Many Nucleon-Hyperon Systems, 26-27 July 2013, KGU Kannai Media Center, Kanto-Gakuin University

**This talk is based on collaboration works which are reported in the following two papers:**

- (1) “ New concept for the ground-state band in  $^{20}\text{Ne}$  within a microscopic cluster model’ ’ ,  
B. Zhou, Z. Z. Ren, C. Xu, Y. Funaki, T. Yamada, A. Tohsaki, H. Horiuchi, P.Schuck, and G. Roepke,  
Phys. Rev. C 86, 014301 (2012),,**
- (2) “ Non-localized clustering: A new concept in nuclear cluster physics’ ’  
B. Zhou, Y. Funaki, H. Horiuchi, Z. Z. Ren, G. Roepke, P.Schuck,  
A. Tohsaki, C. Xu, and T. Yamada,  
Phys. Rev. Lett. 110, 262501 (2013),**

**and also in the following two talks given at**

- (1) RIKEN HPCI international workshop on large-scale computations for nuclear alpha particle condensation  
13 – 19 November 2012, Nishina Center, RIKEN.**
- (2) KITPC/ITP-CAS Program on Clustering Aspects in Nuclei  
1 – 26 April 2013, KITPC/ITP-CAS, Beijing**

# 1. Introduction

Recently the THSR(Tohsaki-Horiuchi-Schuck-Roepke) wave function has proved to be very powerful for the description of cluster-gas states, typically the Hoyle state of  $^{12}\text{C}$ .

$$n\alpha\text{THSR} : \frac{\mathcal{A}\{e^{-\frac{2}{B^2}(\mathbf{X}_1^2 + \dots + \mathbf{X}_n^2)} \phi(\alpha_1) \cdots \phi(\alpha_n)\}}{B = (b^2 + 2R_0^2)^{1/2} \text{ and } \mathbf{X}_i = (1/4) \sum_n \mathbf{r}_{in}}$$

It was found that the the  $3\alpha$  RGM/GCM wave functions of the Hoyle state are almost 100% equivalent to single THSR w.f.'s:

$$|\langle \Phi(\text{single THSR}) | \Psi(3\alpha\text{RGM/GCM}) \rangle|^2 \approx 100\% \quad \text{for Hoyle state}$$

Furthermore, we learned that the  $3\alpha$  RGM/GCM wave functions of the  $^{12}\text{C}$  ground state are about 93 % equivalent to single THSR w.f.'s:

$$|\langle \Phi(\text{single THSR}) | \Psi(3\alpha\text{RGM/GCM}) \rangle|^2 \approx 93\% \quad \text{for } ^{12}\text{C ground state}$$

Ref. Y.Funaki et al., Phys.Rev.C 67,051306(R)(2003)

We also know that  $2\alpha$  RGM/GCM wave functions are 100% equivalent to single THSR w.f.'s

$$|\langle \Phi(\text{single THSR}) | \Psi(2\alpha\text{RGM/GCM}) \rangle|^2 = 100\% \quad \text{for } ^8\text{Be}$$

Ref. Y.Funaki et al., Prog.Theor.Phys. 108, 297(2002)

Recently we have found that the  $^{16}\text{O}-\alpha$  RGM/GCM w.f.'s of the  $K^\pi=(0^\pm)_1$  inversion-doublet-band states of  $^{20}\text{Ne}$  are almost 100 % equivalent to single THSR w.f.'s (at the minimum-energy points of the energy surfaces).

$$|\langle \Phi(\text{single THSR}) | \Psi(^{16}\text{O} + \alpha\text{RGM/GCM}) \rangle|^2 \approx 100\%$$

Ref. B.Zhou et al., Phys.Rev.C 86, 014301(2012), and  
Phys.Rev.Lett. 110, 262501 (2013).

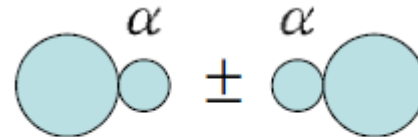
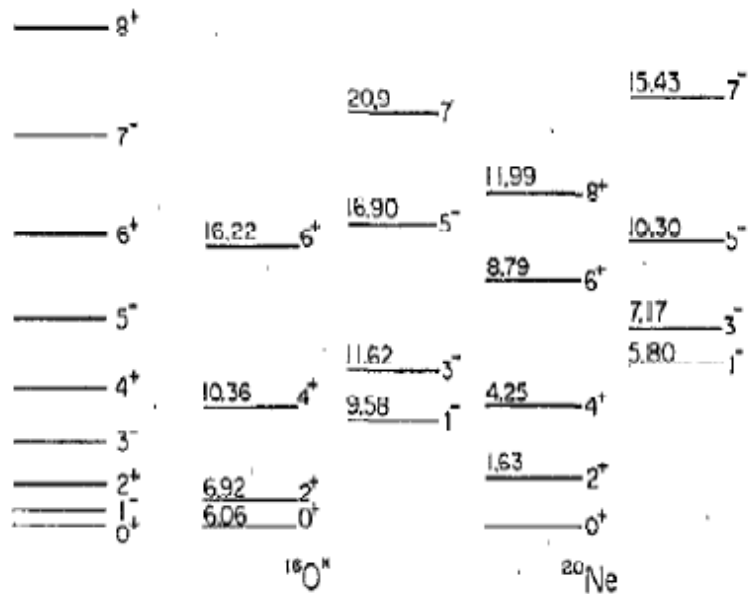
$^{16}\text{O}-\alpha$  THSR wave function

$$\Phi_{\text{THSR}} = \mathcal{A} \left\{ r^L \exp\left[-\frac{8}{5B^2}r^2\right] Y_{LM}(\Omega) \phi(^{16}\text{O}) \phi(\alpha) \right\} \quad (B^2 = b^2 + 2\beta^2 > b^2)$$

In the case of  $8/(5B^2) = (A_1 A_2 / A) (1/(2b^2))$ , under the action of the antisymmetrizer  $\mathcal{A}$ ,  $r^L$  of  $r^L \exp(-\gamma r^2)$  can be replaced by any polynomial of  $r$  of order  $L$  (having order- $L$  monomial  $r^L$ ).  
But for  $8/(5B^2) \neq (A_1 A_2 / A) (1/(2b^2))$ , this replacement is not allowed.

The THSR w.f. is a wave function with no localized clusters.

However, we have long believed that the existence of the  $K^\pi = (0^\pm)_1$  inversion-doublet-band states of  $^{20}\text{Ne}$  is a **verification** of the existence of the **deformed intrinsic state with parity violation** which is naturally satisfied by the spatially localized  $16\text{O}-\alpha$  configuration.



$$^{16}\text{O}^* = ^{12}\text{C} + \alpha$$

$$^{20}\text{Ne} = ^{16}\text{O} + \alpha$$

H.Horiuchi, K.Ikeda

Prog.Theor.Phys. 40, 277 (1968)

Therefore, the above-mentioned result that  $^{20}\text{Ne}$  inversion-doublet-band states are well described by single THSR w.f.'s is very astonishing and it requires us to explain why it is so.

The facts that RGM/GCM solutions are equivalent to single THSR wave functions **in so many typical cluster systems** are not simply astounding but serious.

只事ではない！

Recently it was shown that in 3  $\alpha$  linear chain system, there also holds

$$|\langle \Phi(\text{single THSR}) | \Psi(3\alpha\text{RGM/GCM}) \rangle|^2 \approx 100\%$$

Y.Funaki and T.Suhara

These facts demand us to change our basic understanding of cluster dynamics

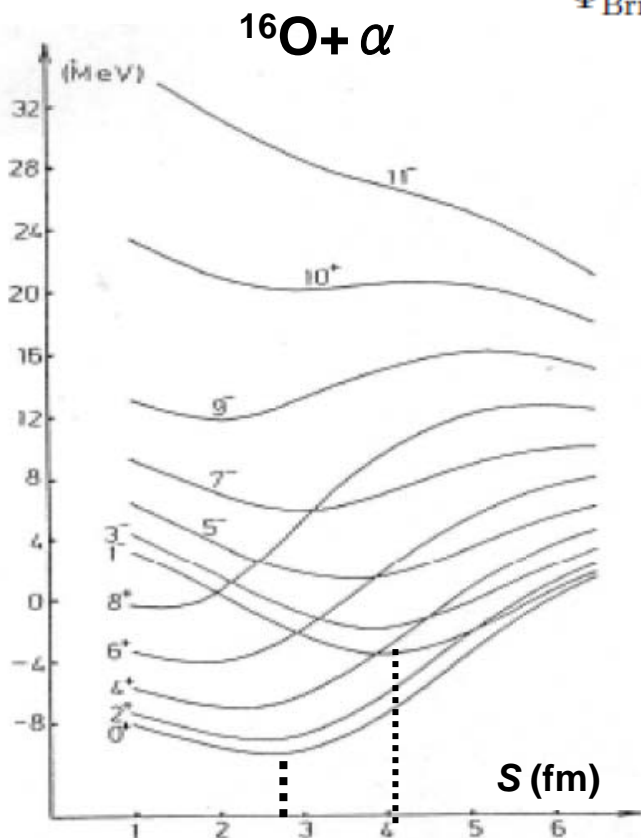
In order to get new understanding (or new concept) of cluster dynamics, we have to clarify every detail of the calculated results by THSR w. f.s including strange-looking properties about deformation.

Clarification of the inversion doublet problem of  $^{20}\text{Ne}$  with THSR wave function is very productive for this purpose.

## 2. Hybrid-Brink-THSR wave function

### (a) Energy curve by Brink w.f.

$$\Phi_{\text{Brink}}(S) = P_{M0}^L \mathcal{A} \left\{ \underbrace{\exp\left[-\frac{8}{5b^2}(r-S)^2\right] \phi(^{16}\text{O}) \phi(\alpha)}_{\text{Slater determinant} / \exp\left(-\frac{10X_G^2}{b^2}\right)} \right\} \quad (S = Se_z)$$



**Brink w.f. has been widely used, since**

Brink w.f. is a Slater determinant, and hence has enabled the microscopic calculation by cluster-model in a wide region of mass number, which was impossible before.

Energy curve for each angular momentum  $L$  has minimum point at non-zero value of the distance parameter  $S$ ,

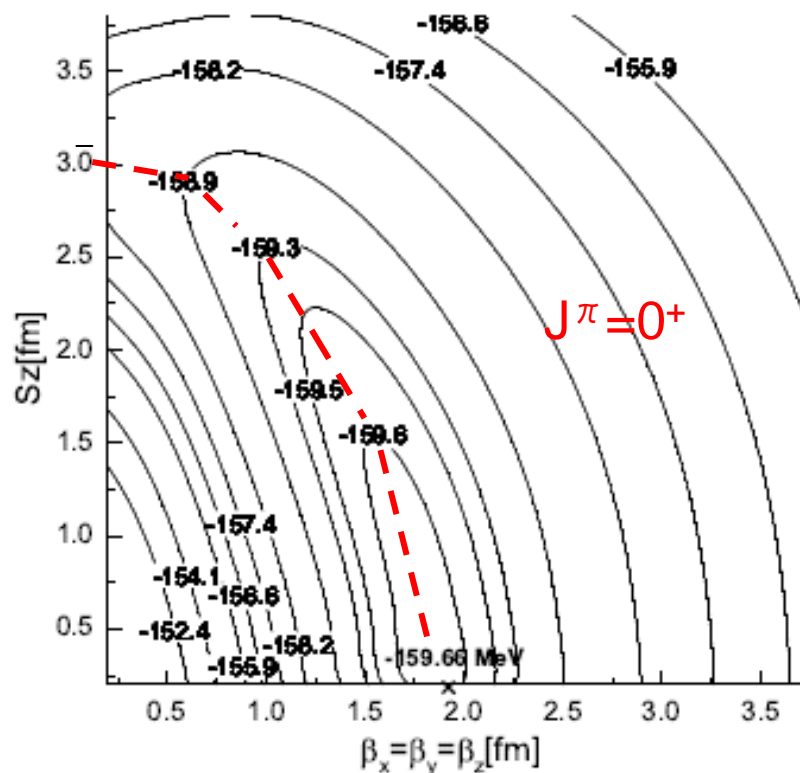
**This fact has supported the concept of localized clustering.**

## (b) Energy curve by Hybrid-Brink-THSR w.f.

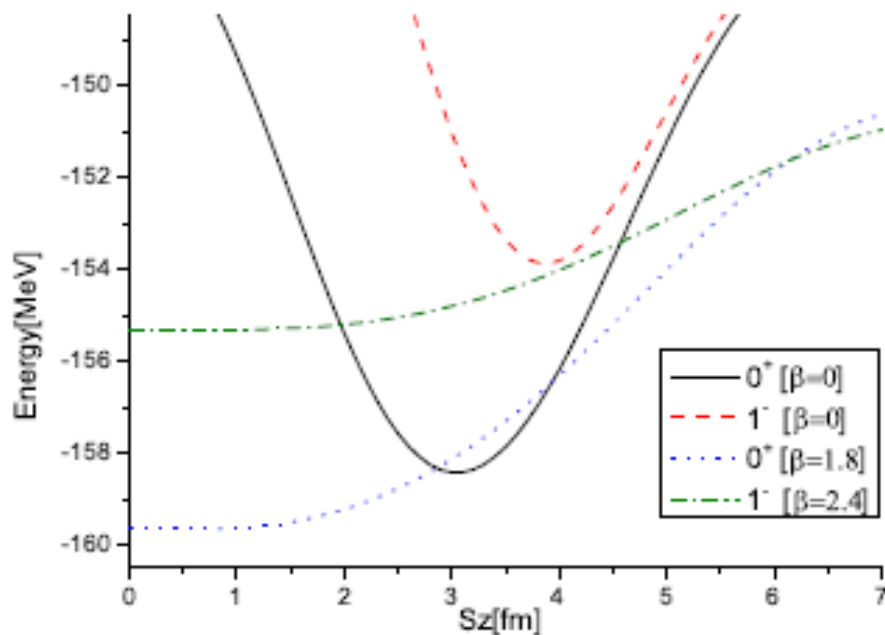
If we use wider width for the relative-motion wave packet than the Brink w.f., the energy curve changes drastically:

$$\mathcal{A} \left[ \exp \left( - \sum_k^{x,y,z} \frac{8(r-S)_k^2}{5B_k^2} \right) \phi(\alpha) \phi(^{16}\text{O}) \right] \quad \underline{B_k^2 = b^2 + 2\beta_k^2}$$

Hybrid-Brink-THSR w.f.



B. Zhou et al.,  
Phys. Rev. Lett. 110, 262501 (2013)



## THSR w.f. with spin $L$ (two-cluster system)

$$\Phi = \mathcal{A} \left\{ \exp[-\gamma(\mathbf{r} - \mathbf{S}_z)^2] \phi(C_1) \phi(C_2) \right\}, \quad \mathbf{S}_z = S \mathbf{e}_z,$$

$$\exp[-\gamma(\mathbf{r} - \mathbf{S}_z)^2] = \exp[-\gamma(r^2 + S^2)] \exp[2\gamma \mathbf{r} \mathbf{S}_z]$$

$$= \exp[-\gamma(r^2 + S^2)] 4\pi \sum_{L=0}^{\infty} i_L(2\gamma S r) \sum_{M=-L}^L Y_{LM}(\hat{\mathbf{r}}) Y_{LM}(\hat{\mathbf{S}}_z)$$

$$\begin{aligned} \Phi_L &= P_{M0}^L \Phi \propto \mathcal{A} \left\{ i_L(2\gamma S r) \exp[-\gamma r^2] Y_{LM}(\hat{\mathbf{r}}) \phi(C_1) \phi(C_2) \right\} \\ &\propto S^L \mathcal{A} \left\{ r^L \exp[-\gamma r^2] Y_{LM}(\hat{\mathbf{r}}) \phi(C_1) \phi(C_2) \right\} + \mathcal{O}(S^{L+2}) \end{aligned}$$

$$\hat{\Phi}_L = \frac{1}{\sqrt{\langle \Phi_L | \Phi_L \rangle}} \Phi_L \propto \frac{1}{S^L \sqrt{\langle \Phi_L^0 | \Phi_L^0 \rangle + \mathcal{O}(S^2)}} \left( S^L \Phi_L^0 + \mathcal{O}(S^{L+2}) \right)$$

$$\Phi_L^0 = \mathcal{A} \left\{ r^L \exp[-\gamma r^2] Y_{LM}(\hat{\mathbf{r}}) \phi(C_1) \phi(C_2) \right\}$$

$$\lim_{S \rightarrow 0} \hat{\Phi}_L = \frac{1}{\sqrt{\langle \Phi_L^0 | \Phi_L^0 \rangle}} \Phi_L^0. \quad \longleftarrow \text{THSR w.f. with spin } L$$

### 3. RGM/GCM w.f. $\approx$ single THSR w.f.

$$|\langle \Phi(\text{single THSR}) | \Psi(^{16}\text{O} + \alpha\text{RGM/GCM}) \rangle|^2 \approx 100\%$$

$K^\pi = (0^+)_1$  band

$^{16}\text{O} - \alpha$

B.Zhou et al., Phys.Rev.C 86, 014301(2012)

State	$E_{\text{Min}}^{\text{Brink}}(R)$	$E_{\text{Min}}^{\text{THSR}}(\beta_x, \beta_z)$	Excited	$E_{\text{GCM}}^{\text{THSR}}(\text{excited})$	Experiment	$ \langle \hat{\Phi}_{\text{Min}}^{\text{THSR}}   \hat{\Phi}_{\text{GCM}}^{\text{Brink}} \rangle ^2$	$ \langle \hat{\Phi}_{\text{Min}}^{\text{THSR}}   \hat{\Phi}_{\text{Min}}^{\text{Brink}} \rangle ^2$
$0^+$	-158.42(3.0)	-159.85(0.9, 2.5)	0	-160.05(0)	-160.64(0)	0.9929	0.9362
$2^+$	-157.19(2.9)	-158.53(0.0, 2.2)	1.33	-158.84(1.21)	-159.01(1.63)	0.9879	0.9494
$4^+$	-154.40(2.6)	-155.50(0.0, 1.8)	4.35	-156.04(4.01)	-156.39(4.25)	0.9775	0.9571
$6^+$	-150.18(2.1)	-150.80(0.0, 1.2)	9.05	-	-151.86(8.78)	-	0.9870
$8^+$	-144.30(1.5)	-144.48(0.0, 0.7)	15.37	-	-148.69(11.95)	-	0.9996

$K^\pi = (0^-)_1$  band

$^{16}\text{O} - \alpha$

B.Zhou et al., Phys.Rev.Lett. 110, 262501 (2013)

State	$E_{\text{Min}}^{\text{Brink}}(R)$	$E_{\text{Min}}^{\text{Hyb}}(\beta_x, \beta_z)$	$E_{\text{GCM}}^{\text{Hyb}}(\text{Excited})$	Experiment	$ \langle \hat{\Phi}_{\text{Min}}^{\text{Hyb}}   \hat{\Phi}_{\text{Min}}^{\text{Brink}} \rangle ^2$	$ \langle \hat{\Phi}_{\text{Min}}^{\text{Hyb}}   \hat{\Phi}_{\text{GCM}}^{\text{Brink}} \rangle ^2$
$1^-$	-153.87(3.9)	-155.38(3.7, 1.4)	-155.38(4.67)	-154.85(5.79)	0.9048	0.9998
$3^-$	-151.40(3.8)	-153.07(3.7, 0.0)	-153.08(6.99)	-153.49(7.16)	0.8863	0.9987
$5^-$	-146.81(3.6)	-148.72(3.3, 0.0)	—	-150.38(10.26)	—	—

The relation, RGM/GCM w.f.  $\approx$  single THSR w.f., has been found to hold in many systems as we already mentioned:

$$^{16}\text{O} + \alpha \text{K}^\pi = (0^\pm)_1, \text{ } ^{12}\text{C Hoyle}, \text{ } ^{12}\text{C ground}, \alpha + \alpha$$

**THSR w.f. expresses non-localized motion of clusters, which is inconsistent with the idea of the parity-violating deformation of localized  $^{16}\text{O} + \alpha$  clustering.**

We have to solve this seeming contradiction.

If we succeed to explain this contradiction, we will have a new understanding of cluster dynamics.

However, “ the characters of the THSR w.f. are not easy to understand, because there holds  
(ProlateTHSR)<sub>J</sub>  $\approx$  (OblateTHSR)<sub>J</sub>  $\approx$  (SphericalTHSR)<sub>J</sub>.

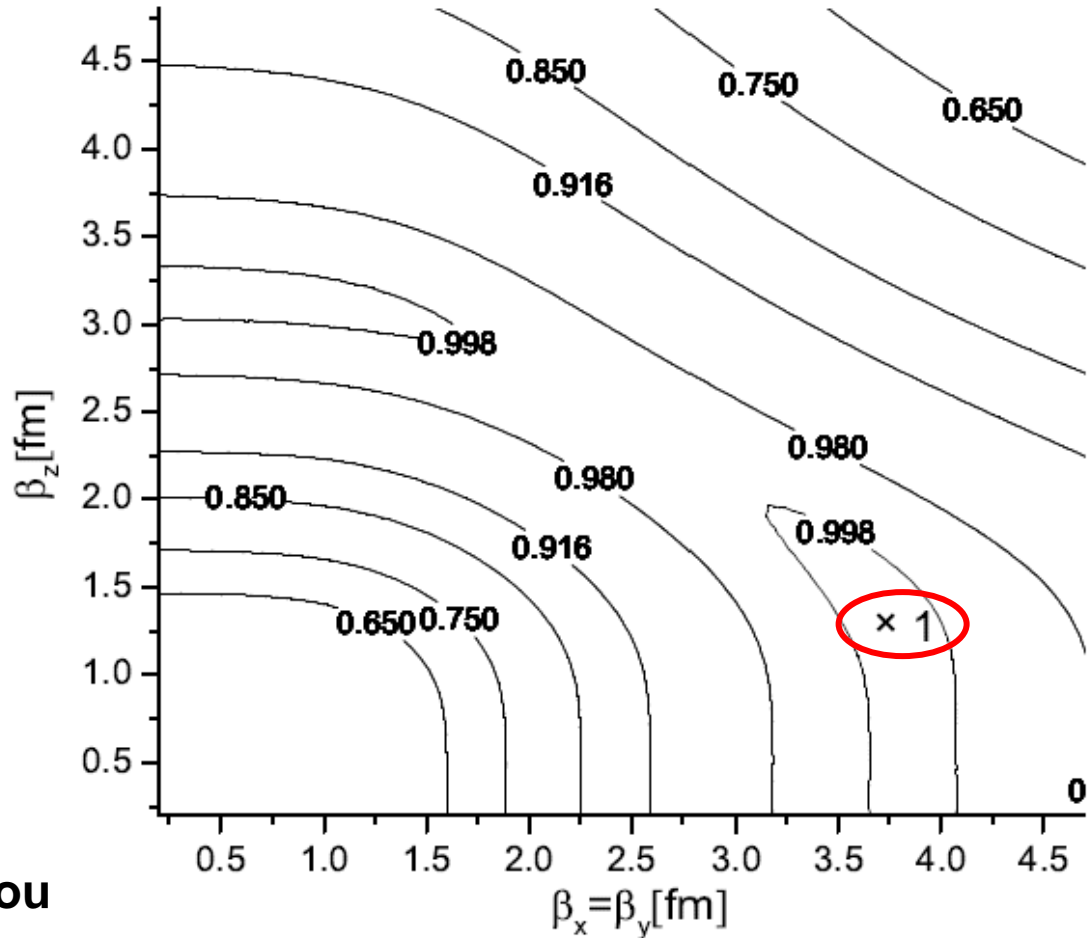
This relation looks like as if there exists no definite deformation and no definite intrinsic state.

Thus, we have to clarify the characters of the THSR w.f..

# 4. (ProlateTHSR)<sub>J</sub> ≈ (OblateTHSR)<sub>J</sub> ≈ (SphericalTHSR)<sub>J</sub>

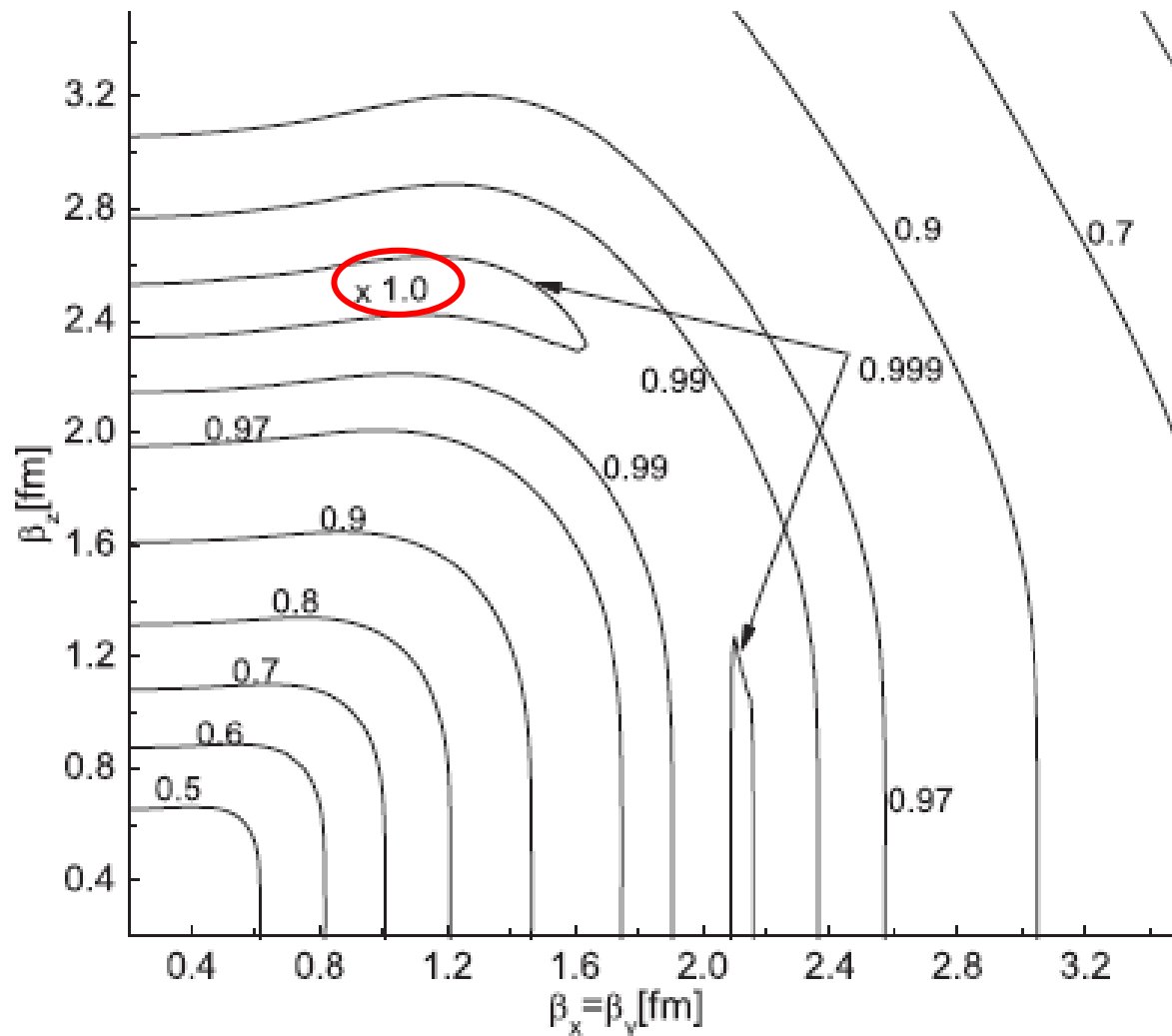
Squared overlap of THSR( $s_z=0.01, \beta_x=3.7, \beta_z=1.4$ )  
 with THSR( $s_z=0.01, \beta_x, \beta_z$ ) for  $1^-$  state of  $^{20}\text{Ne}$

$^{16}\text{O}+$   
 $J^\pi = 1^-$



B.Zhou

B. Zhou et al.,  
Phys. Rev. C.86,  
014301 (2012)

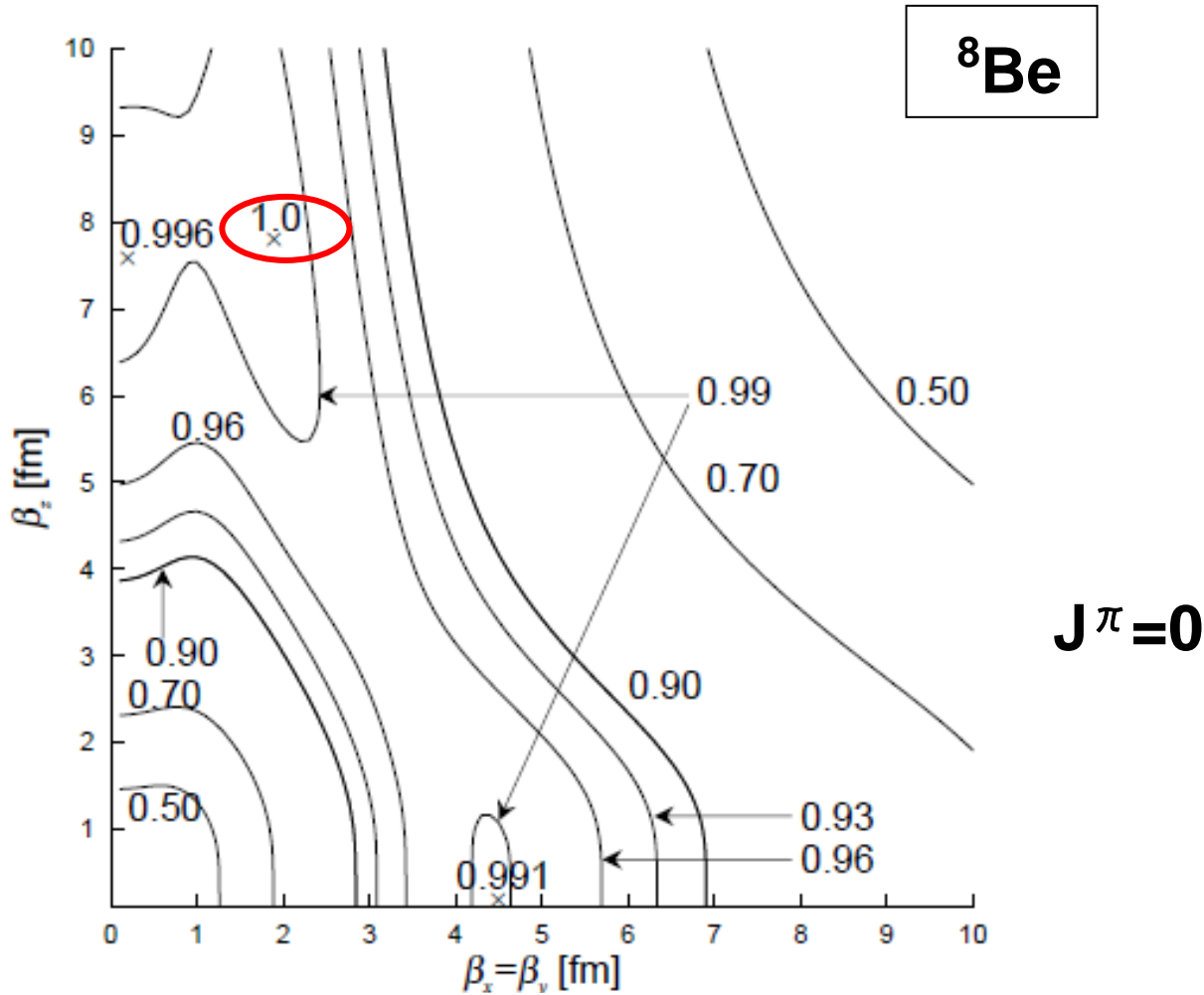


$J^\pi = 0$

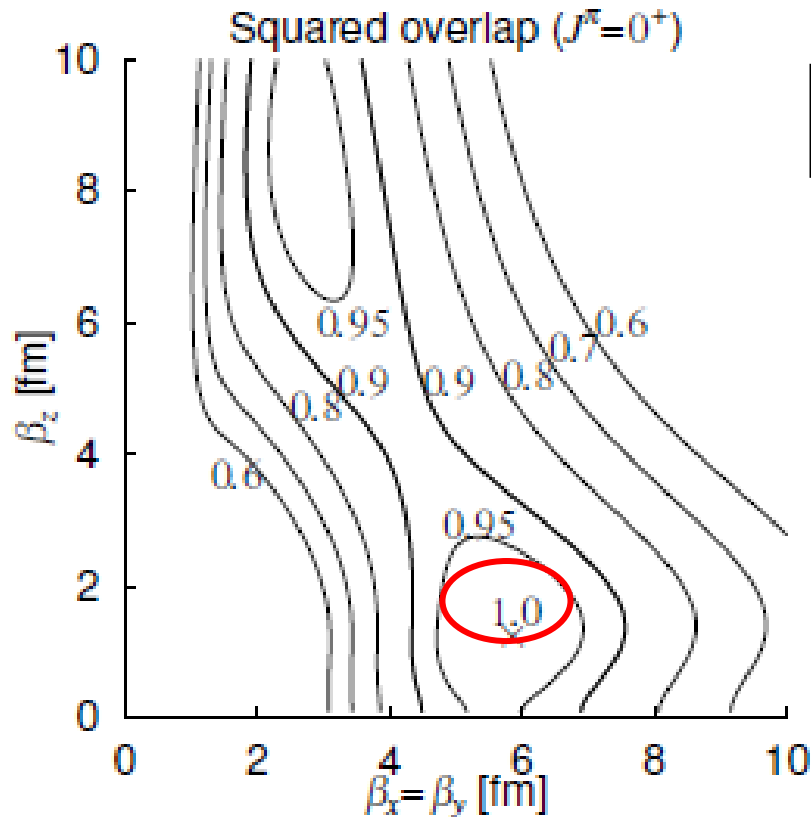
$^{20}\text{Ne}$

FIG. 4. Contour map of the squared overlap between the  $0^+$  wave function with  $\beta_x = \beta_y = 0.9$  fm and  $\beta_z = 2.5$  fm and the  $0^+$  wave function with variable  $\beta_x (= \beta_y)$  and  $\beta_z$ . Numbers on the contour lines are squared overlap values.

Squared overlap of  $0^+$  THSR ( $\beta_x=1.8, \beta_z=7.8$ ) with  $0^+$  THSR( $\beta_x, \beta_z$ )



# Squared overlap of $0^+$ THSR ( $\beta_x=5.7, \beta_z=1.3$ ) with $0^+$ THSR( $\beta_x, \beta_z$ )



3

$J^\pi=0$

Y.Funaki et al.,

Eur. Phys. J. A 24, 321–342 (2005)

**Fig. 1.** Contour map of the squared overlap,  $|\langle \hat{\Phi}_{3\alpha}^{N, J=0}(\beta) | \hat{\Phi}_{3\alpha}^{N, J=0}(\beta_1) \rangle|^2$ , in the two-parameter space,  $\beta_x (= \beta_y)$  and  $\beta_z$ , where  $\beta_1 = (\beta_x = \beta_y = 5.7 \text{ fm}, \beta_z = 1.3 \text{ fm})$ . The harmonic-oscillator size parameter  $b = 1.35 \text{ fm}$ .

# $n\alpha$ THS

$$\widehat{\Phi}_{n\alpha}(\beta) = \mathcal{A} \left[ \exp \left\{ -2 \sum_{i=1}^{n-1} \mu_i \left( \frac{\xi_{ix}^2 + \xi_{iy}^2}{B_x^2} + \frac{\xi_{iz}^2}{B_z^2} \right) \right\} \phi^n(\alpha) \right]$$

$$\begin{cases} \xi_i = X_{i+1} - \frac{1}{i} \sum_{j=1}^i X_j, \\ X_G = \frac{1}{n} \sum_{j=1}^n X_j, \\ \mu_i = \frac{i}{i+1}, \quad (i = 1, \dots, n-1). \end{cases}$$

$$\begin{aligned} \frac{\xi_{ix}^2 + \xi_{iy}^2}{B_x^2} + \frac{\xi_{iz}^2}{B_z^2} &= \left( \frac{2}{3B_x^2} + \frac{1}{3B_z^2} \right) \xi_i^2 + \left( \frac{1}{3B_z^2} - \frac{1}{3B_x^2} \right) \\ &\times (2\xi_{iz}^2 - \xi_{ix}^2 - \xi_{iy}^2) = \end{aligned}$$

$$\left( \frac{2}{3B_x^2} + \frac{1}{3B_z^2} \right) \xi_i^2 + \left( \frac{1}{3B_z^2} - \frac{1}{3B_x^2} \right) \sqrt{\frac{16\pi}{5}} \xi_i^2 Y_{20}(\widehat{\xi}_i),$$

Y.Funaki et al.,

Eur. Phys. J. A **24**, 321–342 (2005)

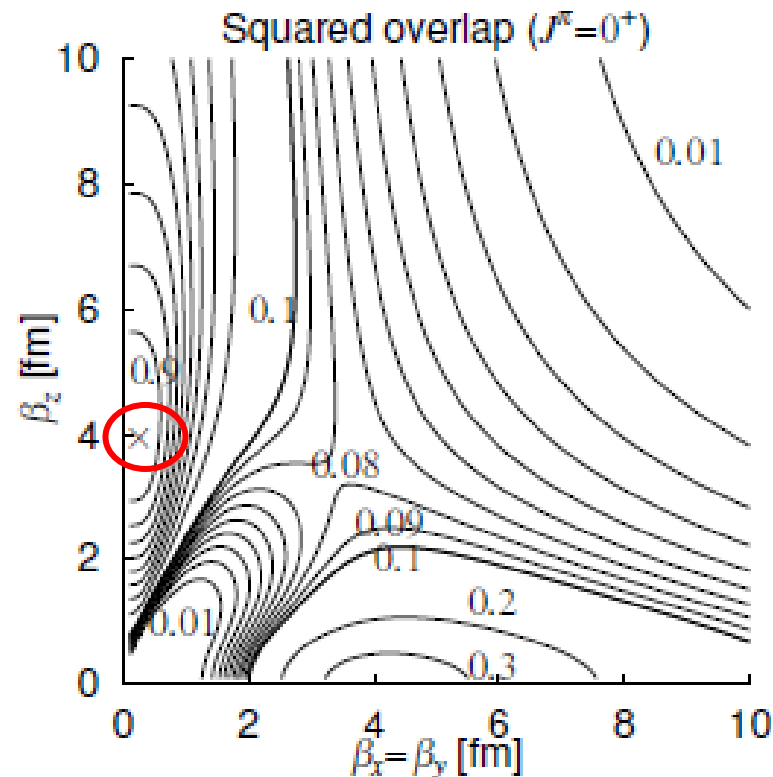
Angular-momentum projection gives following dominant forms:

for  $J = 0$ , 
$$\mathcal{A} \left[ \exp \left\{ -2 \left( \frac{2}{3B_x^2} + \frac{1}{3B_z^2} \right) \sum_{i=1}^{n-1} \mu_i \xi_i^2 \right\} \phi^n(\alpha) \right]$$

for  $J = 2$ , 
$$\mathcal{A} \left[ \exp \left\{ -2 \left( \frac{2}{3B_x^2} + \frac{1}{3B_z^2} \right) \sum_{i=1}^{n-1} \mu_i \xi_i^2 \right\} \right. \\ \left. \times \sum_{i=1}^{n-1} \mu_i \xi_i^2 Y_{20}(\widehat{\xi}_i) \phi^n(\alpha) \right].$$

**These forms are the same for both prolate ( $B_z > B_x$ ) and oblate ( $B_z < B_x$ ) defs..**

For 3  $\alpha$ -linear-chain THSR, there exists no oblate THSR which has large overlap with it.



Y.Funaki et al.,  
Eur.Phys.J A24,  
321 (2005).

**Fig. 2.** Contour map of the squared overlap,  $|\langle \hat{\Phi}_{3\alpha}^{N,J=0}(\beta) | \hat{\Phi}_{3\alpha}^{N,J=0}(\beta_L) \rangle|^2$ , in the two-parameter space,  $\beta_x (= \beta_y)$  and  $\beta_z$ , where  $\beta_1 = (\beta_x = \beta_y = 0.1 \text{ fm}, \beta_z = 4.0 \text{ fm})$ . The harmonic-oscillator size parameter  $b = 1.35 \text{ fm}$ .

## 5. Physical oblate deformation does not exist in $^{16}\text{O} + \alpha$ THSR and the reason of it

$^{16}\text{O} + \alpha$  RGM/GCM w.f.'s are equivalent to single THSR w.f.'s. Since  $^{16}\text{O} + \alpha$  GCM w.f.'s have prolate intrinsic states, the THSR w.f.'s are regarded as having prolate deformation even for  $(\text{oblateTHSR})_J$ .

Since  $(\text{prolateTHSR})_J = (\text{oblateTHSR})_J$ , there holds  $\langle (\text{prolateTHSR})_J | Q | (\text{prolateTHSR})_J \rangle = \langle (\text{oblateTHSR})_J | Q | (\text{oblateTHSR})_J \rangle$ , where  $Q$  is  $Q$ -moment operator.

According to the formula,  $\langle J | Q | J \rangle = -J/(2J+3) \cdot Q_{\text{int}}$ , prolate deformation with  $Q_{\text{int}} > 0$  gives  $\langle J | Q | J \rangle < 0$ .

**We can prove that arbitrary RGM w.f. gives  $\langle J | Q | J \rangle < 0$ , which means prolate deformation.**

Although the oblate THSR w.f. has oblate density distribution, its projected w.f.  $(\text{oblateTHSR})_J$  is prolate !!

What is happening ?

We can prove that any system of two SU(3)-scalar clusters has prolate deformation.

<PROOF>

With arbitrary  $\chi(r)$

$$\Psi = A \{ \chi(r) Y_{LM}(\Omega) \Phi(C_1) \Phi(C_2) \}$$

$$\begin{aligned} \langle \Psi | (1/2) \sum_i Q(i) | \Psi \rangle & \quad \{ Q(i) = Q_{20}(r_i - r_G), \quad Q_{20}(r) = 3z^2 - r^2 \} \\ & = (1/2) (16\pi/5)^{1/2} \langle Y_{LL}(\Omega) | Y_{20}(\Omega) | Y_{LL}(\Omega) \rangle (A_1 A_2 / A) \langle r^2 \rangle_{\text{relative}} \\ & = - (L/(2L+3)) (A_1 A_2 / A) \langle r^2 \rangle_{\text{relative}} < 0. \end{aligned}$$

$$\begin{aligned} (A_1 A_2 / A) \langle r^2 \rangle_{\text{relative}} & = \langle \Psi | \sum_i (r_i - r_G)^2 | \Psi \rangle \\ & \quad - \langle \Phi(C_1) | \sum_{i \in C_1} (r_i - r_{C_1})^2 | \Phi(C_1) \rangle \\ & \quad - \langle \Phi(C_2) | \sum_{i \in C_2} (r_i - r_{C_2})^2 | \Phi(C_2) \rangle \end{aligned}$$

From this result we have

$$\begin{aligned} Q(\text{int}) & = (A_1 A_2 / A) \langle r^2 \rangle_{\text{relative}} \\ & = \langle \Psi | \sum_i (r_i - r_G)^2 | \Psi \rangle - \langle \Phi(C_1) | \sum_{i \in C_1} (r_i - r_{C_1})^2 | \Phi(C_1) \rangle \\ & \quad - \langle \Phi(C_2) | \sum_{i \in C_2} (r_i - r_{C_2})^2 | \Phi(C_2) \rangle \end{aligned}$$

$$3.2 = 16 \cdot 4 / 20$$

Table 1: Check of Matsuse-Kamimura-Fukushima. H and V stand for HNY and Volkov potentials.  $Q(\text{int})_F = 3.2R^2$  with  $R^2 = \langle \Psi | r^2 | \Psi \rangle_{\text{relative}}$ .  $Q(\text{int})$  H and  $Q(\text{int})$  V are calculated from  $Q(L)$  by using  $Q(L) = -[L/(2L + 3)]Q(\text{int})$  with  $Q(L) = \langle \Psi | (1/2) \sum_i Q_{20}(i) | \Psi \rangle$ .

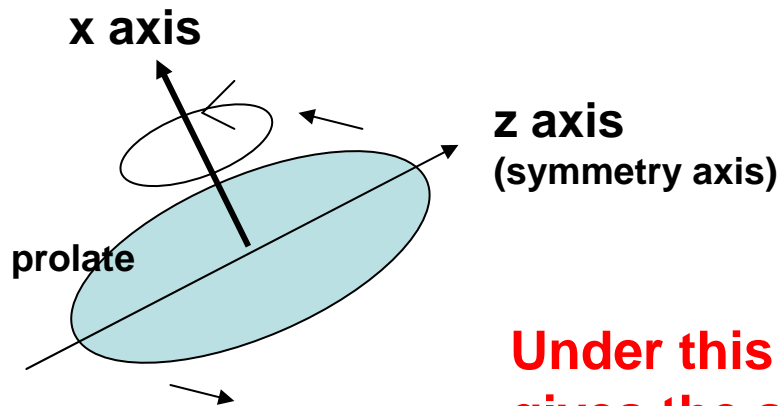
$L^\pi$	$\sqrt{R^2}$ H	$Q(\text{int})$ H	$Q(\text{int})_F$	$\sqrt{R^2}$ V	$Q(\text{int})$ V	$Q(\text{int})_F$
$2^+$	3.64	42.5	42.4	4.00	51.3	51.2
$4^+$	3.55	40.4	40.3	3.90	48.7	48.7
$6^+$	3.41	37.1	37.2	3.69	43.6	43.6
$8^+$	3.22	33.1	33.2	3.37	36.3	36.3
$1^-$	4.49	66.6	64.5	4.68	73.5	70.1
$3^-$	4.55	67.3	66.2	4.78	74.2	73.1
$5^-$	4.53	66.2	65.7	4.77	73.3	72.8
$7^-$	4.43	62.9	62.8	4.69	70.4	70.4
$9^-$	4.17	55.6	55.6	4.48	64.2	64.2

T.Matsuse, M.Kamimura, and Y.Fukushima,  
Prog. Theor. Phys. 53, 706 (1975).

**Rather large deviations of  $Q(\text{int})$  of Matsuse et al. for  $L^\pi = 1^-, 3^-, 5^-$  states from the formula  $Q(\text{int}) = (A_1 A_2 / A) \langle r^2 \rangle_{\text{relative}}$  are due to the modification of the tail parts of these resonance wave functions with broad widths by connecting them smoothly with irregular Coulomb waves  $G_L(kr)$ .**

In angular momentum projection, the Intrinsic wave function is rotated.

Therefore, we can conjecture that the oblate THSR is equivalent to the rotation average of a prolate THSR around an axis perpendicular to its symmetry axis.



Rotation average of a prolate THSR results in oblate THSR

$$\mathcal{N} \frac{1}{2\pi} \int_0^{2\pi} d\theta e^{-i\theta L_x} \Phi_{\text{prol}} = \Phi_{\text{obl}}$$

Under this relation, angular-momentum projection gives the same w.f.:

$$n P^{L,M} \Phi_{\text{obl}} = n' P^{L,M} \Phi_{\text{prol}}$$

$$\Phi = \left( \frac{1}{2\pi} \int d\theta e^{-i\theta \ell_x} \right) \exp \left\{ -\frac{r_x^2 + r_y^2}{B_x^2} - \frac{r_z^2}{B_z^2} \right\} \approx \exp \left\{ -\frac{r_x^2}{B_x'^2} - \frac{r_y^2 + r_z^2}{B_y'^2} \right\}$$

$$\frac{1}{B_x'^2} = \frac{1}{B_x^2} \quad \frac{1}{B_y'^2} = \frac{1}{2} \left\{ \frac{1}{B_x^2} + \frac{1}{B_z^2} \right\}$$

↑  
in the first order of  $(B_x^2 - B_z^2)$

# $^{20}\text{Ne}$ case

$\Psi^{THSR}(\beta_x, \beta_y, \beta_z)$ : THSR w.f. before Ang. Mom. Proj.

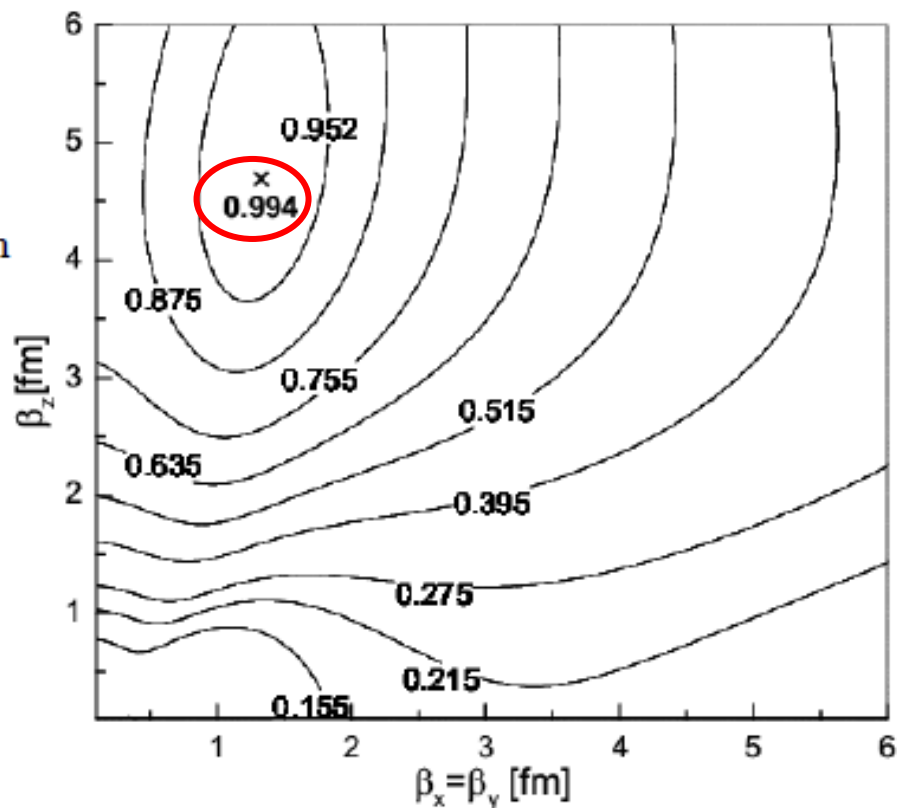
$$f_{\text{overlap}}(\beta_{\perp}, \beta_z; \tilde{\beta}_{\perp}, \tilde{\beta}) = N \left\langle \Psi^{THSR}(\tilde{\beta}, \tilde{\beta}_{\perp}, \tilde{\beta}_{\perp}) \left| \int_0^{2\pi} d\theta e^{-iJ_z \theta} \Psi^{THSR}(\beta_{\perp}, \beta_{\perp}, \beta_z) \right. \right\rangle$$

$$N = \left( \left\langle \Psi^{THSR}(\tilde{\beta}, \tilde{\beta}_{\perp}, \tilde{\beta}_{\perp}) \left| \Psi^{THSR}(\tilde{\beta}, \tilde{\beta}_{\perp}, \tilde{\beta}_{\perp}) \right. \right\rangle \left\langle \int_0^{2\pi} d\theta e^{-iJ_z \theta} \Psi^{THSR}(\beta_{\perp}, \beta_{\perp}, \beta_z) \left| \int_0^{2\pi} d\theta e^{-iJ_z \theta} \Psi^{THSR}(\beta_{\perp}, \beta_{\perp}, \beta_z) \right. \right\rangle \right)^{-1/2}$$

$$|f_{\text{overlap}}(\beta_{\perp}, \beta_z; \tilde{\beta}_{\perp}, \tilde{\beta})|^2$$

for  $(\tilde{\beta}, \tilde{\beta}_{\perp}, \tilde{\beta}_{\perp}) = (1.4, 3.7, 3.7)$ ,

which corresponds to **1** minimum after Ang. Mom. Proj.

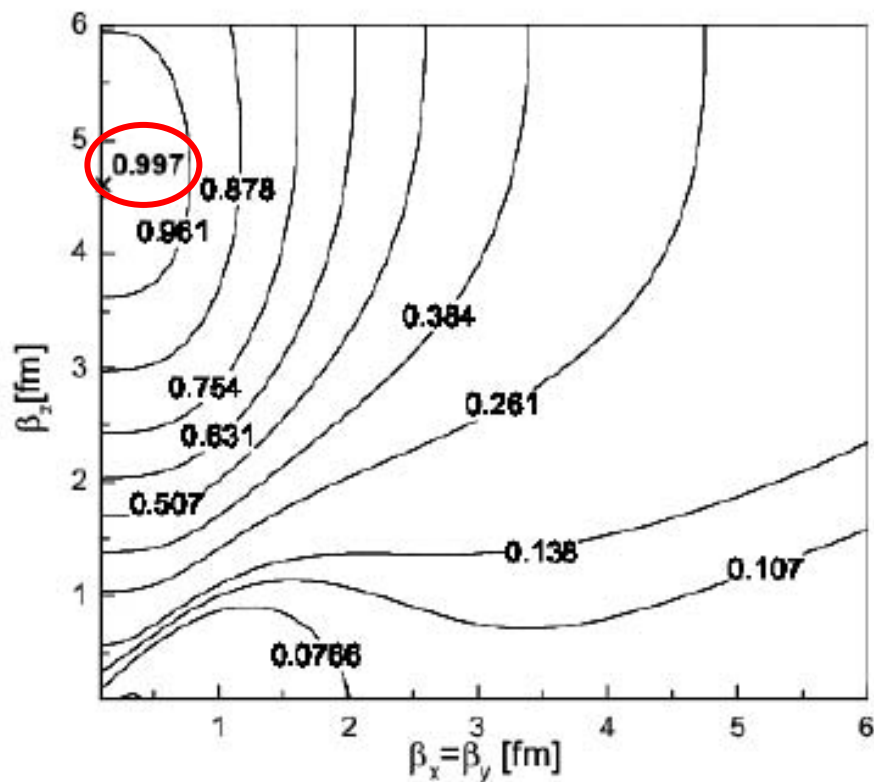


B.Zhou

$$|f_{overlap}(\beta_{\perp}, \beta_z; \tilde{\beta}_{\perp}, \tilde{\beta})|^2$$

for  $(\tilde{\beta}, \tilde{\beta}_{\perp}, \tilde{\beta}_{\perp}) = (0.01, 3.7, 3.7)$ ,

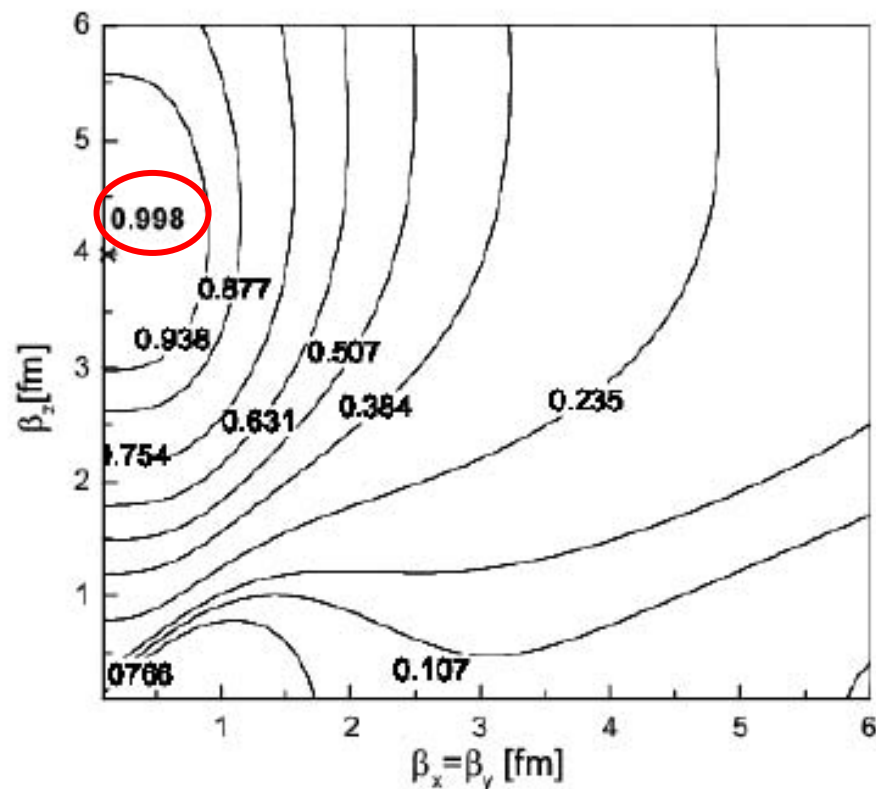
which corresponds to **3<sup>+</sup>** minimum  
after Ang. Mom. Proj.



$$|f_{overlap}(\beta_{\perp}, \beta_z; \tilde{\beta}_{\perp}, \tilde{\beta})|^2$$

for  $(\tilde{\beta}, \tilde{\beta}_{\perp}, \tilde{\beta}_{\perp}) = (0.01, 3.3, 3.3)$ ,

which corresponds to **5<sup>+</sup>** minimum  
after Ang. Mom. Proj.

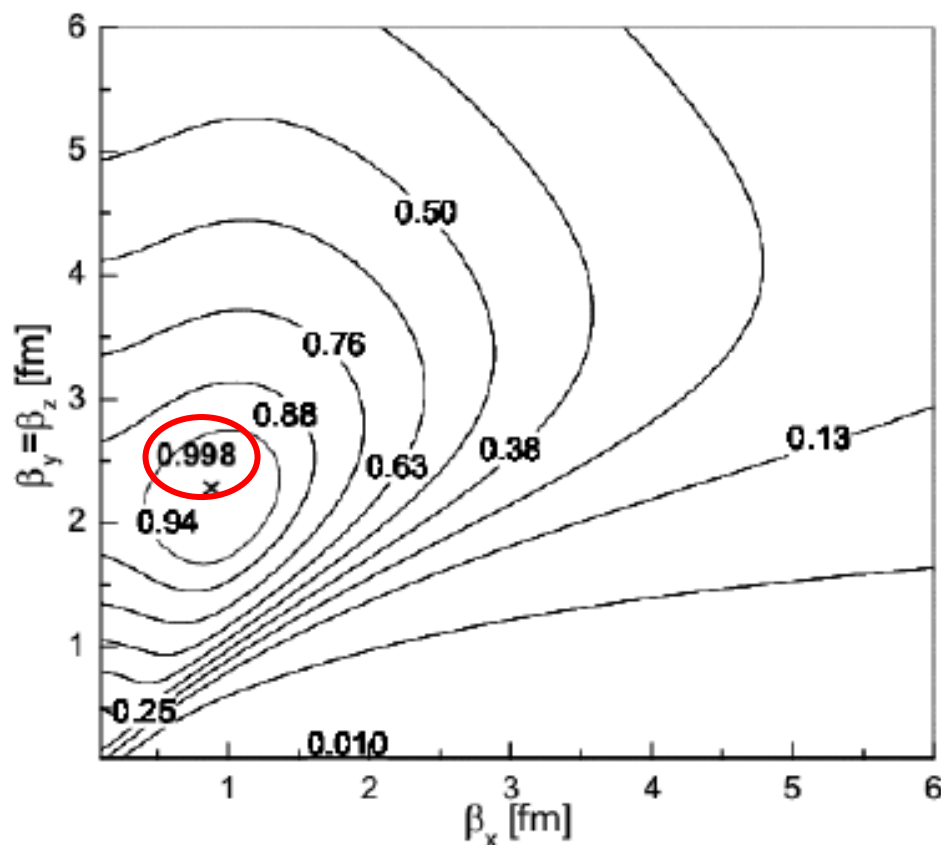


$$f'_{overlap}(\beta_x, \beta_\perp; \tilde{\beta}_\perp, \tilde{\beta}_z) = N \left\langle \Psi^{THSR}(\beta_x, \beta_\perp, \beta_\perp) \left| \int_0^{2\pi} d\theta e^{-iJ_z \theta} \Psi^{THSR}(\tilde{\beta}_\perp, \tilde{\beta}_\perp, \tilde{\beta}_z) \right. \right\rangle$$

$$N = \left( \left\langle \Psi^{THSR}(\tilde{\beta}_\perp, \tilde{\beta}_\perp, \tilde{\beta}_z) \left| \Psi^{THSR}(\tilde{\beta}_\perp, \tilde{\beta}_\perp, \tilde{\beta}_z) \right. \right\rangle \left\langle \int_0^{2\pi} d\theta e^{-iJ_z \theta} \Psi^{THSR}(\beta_x, \beta_\perp, \beta_\perp) \left| \int_0^{2\pi} d\theta e^{-iJ_z \theta} \Psi^{THSR}(\beta_x, \beta_\perp, \beta_\perp) \right. \right\rangle \right)^{-1/2}$$

B.Zhou

$|f'_{overlap}(\beta_x, \beta_\perp; \tilde{\beta}_\perp, \tilde{\beta}_z)|^2$   
 for  $(\tilde{\beta}_\perp, \tilde{\beta}_\perp, \tilde{\beta}_z) = (0.9, 0.9, 2.5)$ ,  
 which corresponds to  $0^+$  minimum  
 after Ang. Mom. Proj.



# Chain of rotation averaging

**Rotation averaging makes deformation smaller.**

In the first order approximation of the deformation ( $B_x - B_z$ ), we have

$$\left. \begin{aligned} \frac{1}{B_x'^2} &= \frac{1}{B_x^2} \\ \frac{1}{B_y'^2} &= \frac{1}{2} \left\{ \frac{1}{B_x^2} + \frac{1}{B_z^2} \right\} \end{aligned} \right\} \longrightarrow \frac{1}{B_x'^2} - \frac{1}{B_y'^2} = \frac{1}{2} \left\{ \frac{1}{B_x^2} - \frac{1}{B_z^2} \right\}$$

**However, two wave functions  $\Phi_{AV}$  and  $\Phi$  related by rotation averaging,**

$$\Phi_{AV} = R_{AV} \Phi \quad R_{AV} = \left( \frac{1}{2\pi} \int d\theta e^{-i\theta \ell_x} \right)$$

**are identical with each other after angular-momentum projection.**

$$n_{AV} P^{L,M} \Phi_{AV} = n P^{L,M} \Phi$$

**Therefore, for example, the energies by these projected w.f.'s are the same.**

**From these facts, if we start with a THSR w/f.  $\Phi$ , even if  $R_{AV} \Phi$  is well-approximated by some single THSR w.f.,**

**$(R_{AV})^2 \Phi$  or  $(R_{AV})^3 \Phi$  is considered to be not so well approximated by some single THSR w.f..**

# $^8\text{Be}$

<b>(6.5、6.5. 0.1) Obl</b>	<b>Rot-Av</b>	<b>⇒</b>	<b>(1.8、1.8、7.8)Prol</b>	<b>0.8473</b>
<b>(1.8、1.8、7.8)Prol</b>	<b>Rot-Av</b>	<b>⇒</b>	<b>(1.9、4.5. 4.5)Obl</b>	<b>0.9725</b>
<b>(1.9、4.5. 4.5) Obl</b>	<b>Rot-Av</b>	<b>⇒</b>	<b>(4.6、3.0、3.0)Prol</b>	<b>0.9944</b>
<b>(0.1、4.4、4.4) Obl</b>	<b>Rot-Av</b>	<b>⇒</b>	<b>(4.6、2.1、2.1)Prol.</b>	<b>0.9363</b>

## **6. Container picture for cluster structure and effectively-localized clustering**

**The C.M. motions of clusters in THSR w.f. are mutually independent and are described by Gaussian wave packets which are non-localized and are characterized by size parameters  $B$  of the magnitude of nuclear radius.**

**The cluster dynamics by the THSR w.f. is described not by the inter-cluster distance parameter but by the size parameter  $B$  of the system-container potential whose lowest orbits are occupied by the clusters.**

**We may call this description of the cluster dynamics the container picture of cluster dynamics.**

**The word 'container' means the self-consistent mean field of clusters with the stress on its character that the central quantity of the mean field is the system size.**

**For instance, the excitation of the system is described firstly by the dynamics of the size parameter  $B$  which is adopted as the generator coordinate and then by the excitation of the single-particle motion of clusters in the container.**

**This naming may sound more appropriate for three-cluster systems because, for example, in the  $3\alpha$  system it describes the ground state and  $3\alpha$ -gas states on the same footing.**

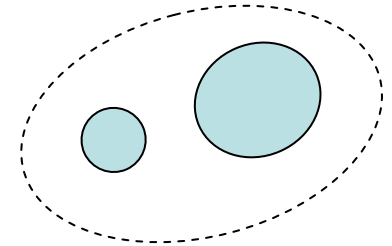
**In this picture, the existence of cluster-gas state is very natural and the formation mechanism of cluster-gas states from the ground state is just the dilatation (density decrease) which can be well described by the size parameter  $B$  of the system container.**

**Now we explain how the idea of the parity-violating deformation of localized  $^{16}\text{O} + \alpha$  clustering is justified in this container picture.**

**The parity-violating deformation is a property of the intrinsic state which is the instantaneous (or adiabatic) quantum state of the rotation of the nucleus.**

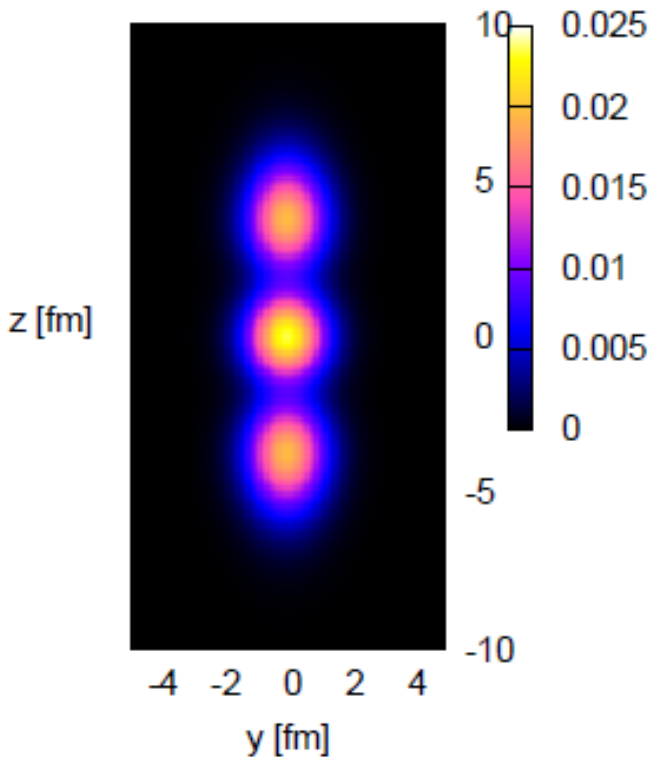
Since the instantaneous configuration of two clusters is of prolate shape, the prolate THSR is the intrinsic state of the system and the oblate THSR is not the intrinsic state but rather a mathematical object which expresses the rotation-average of the intrinsic state. The spherical THSR expresses the time average of the rotational motion, namely the angular-momentum projected state of the intrinsic state (the prolate THSR).

Since two clusters can not come close to each other because of inter-cluster Pauli exclusion, two clusters in the intrinsic state (the prolate THSR) is effectively localized in space. Thus, the prolate THSR has the parity-violating deformation of localized  $^{16}\text{O} + \alpha$  clustering.



We can say that dynamics prefers non-localized clustering but kinematics makes the system look like localized clustering.

The effective localization of clusters in the prolate THSR w.f. is clearly seen in the density distribution of the prolate THSR of  $2\alpha$  :

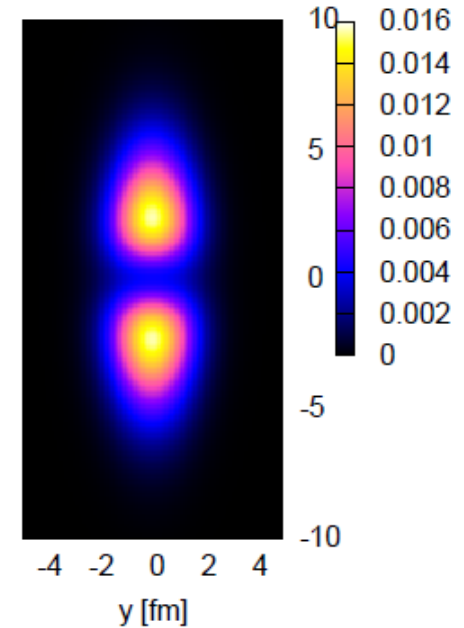


$2\alpha$  THSR:

$$\beta_x = \beta_y = 1.78 \text{ fm}$$

$$\beta_z = 7.85 \text{ fm } (b=1.37\text{fm})$$

$z$  [fm]



$3\alpha$  THSR:

$$\beta_x = \beta_y = 0.01 \text{ fm,}$$

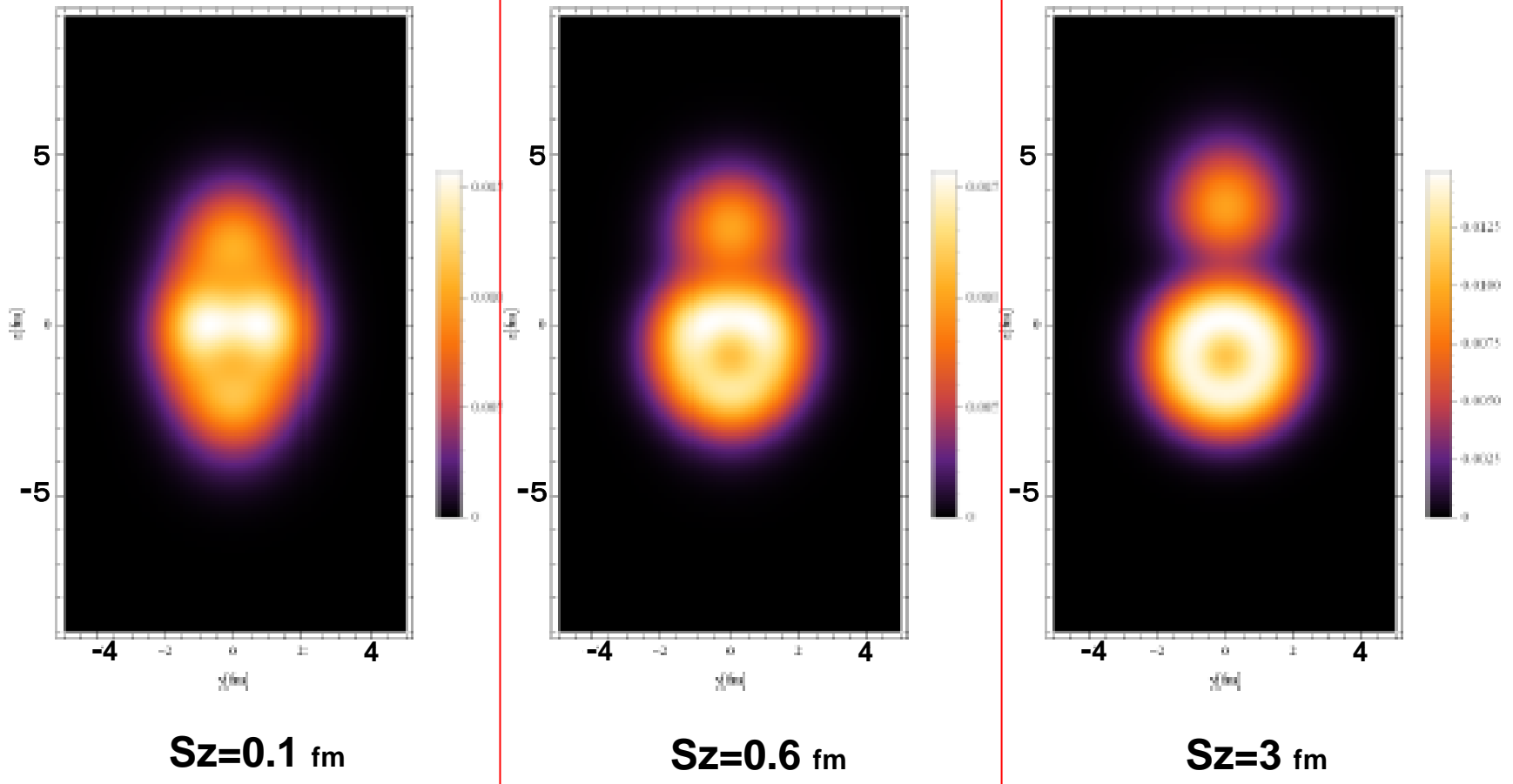
$$\beta_z = 5.1 \text{ fm}$$

A more interesting verification of the effective localization of clusters is given by the density distribution of  $3\alpha$  THSR w.f. with strong prolate deformation.

Y.Funaki  
and T.Suhara

$$|\langle \Phi(\text{single THSR}) | \Psi(3\alpha\text{RGM/GCM}) \rangle|^2 \approx 100\%$$

( $3\alpha$  linear chain)



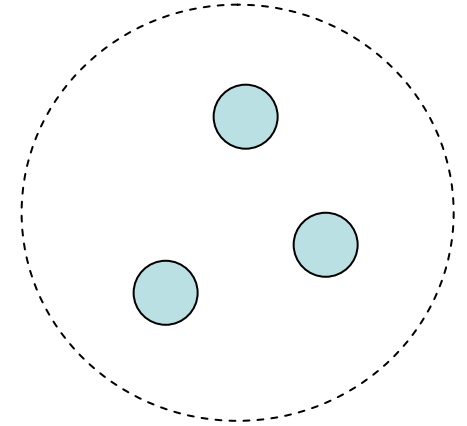
**Sz=0.6 fm is much smaller than inter-cluster distance  $\approx$  3 fm.**

Figure 5: (Left): The density profile for the intrinsic hybrid wave function with  $S_z=0.1\text{fm}$ , that is,  $\rho_{\text{int}}(x=0, y, z; \beta_x=0.9, \beta_z=2.5, S_z=0.1)$ . (Middle): The density profile for the intrinsic hybrid wave function with  $S_z=0.6\text{fm}$ , that is,  $\rho_{\text{int}}(x=0, y, z; \beta_x=0.9, \beta_z=2.5, S_z=0.6)$ . (Right): The density profile for the intrinsic hybrid wave function with  $S_z=3\text{fm}$ , that is,  $\rho_{\text{int}}(x=0, y, z; \beta_x=0.9, \beta_z=2.5, S_z=3)$ .

**In three or more cluster systems, we need to note that the inter-cluster separations are non-zero simultaneously.**

**In general, the spatial arrangement of clusters are not necessarily geometrical, namely clusters are non-localised, except some special cases such as strongly- prolate deformation discussed above.**

**When the inter-cluster separations are large, the spatial arrangement of clusters can be non-rigid and gas-like**



**A very important merit of the container picture of clustering is that it explains the ground state and cluster-gas states on the same footing. In this picture, the existence of cluster-gas state is very natural ! The formation mechanism of cluster-gas states from the ground state is just the dilatation (density decrease) as we expected.**

## 7. Summarizing discussions

Description of the cluster structure has been made by the use of either the inter-cluster relative w.f. (RGM) or by the inter-cluster distance parameter (BrinkGCM).

Now THSR study says that **system-size (or density) parameter** is important for describing cluster structure.

We can say that the ground state has the structure where two clusters are put in a **self-consistent container** of H.O. potential type.

(Of course the system is under the strong influence of Pauli Principle.)

This new picture of clustering may be called container picture of clustering. **The word 'container' is chosen because it stresses that the central quantity of cluster dynamics is the system size.**

This picture explains the ground state with effectively-localized clusters and cluster-gas states on the same footing.

**The existence of cluster-gas state is very natural in this picture.**

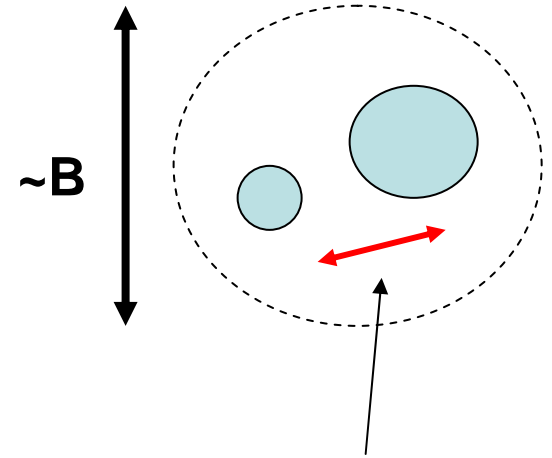
*The formation mechanism of cluster-gas states from the ground state is just the dilatation (density decrease) as we expected.*

Dynamics prefers non-localized clustering but inter-cluster Pauli principle makes the system look like localized clustering in two-cluster systems not only in the ground state but also in excited states.

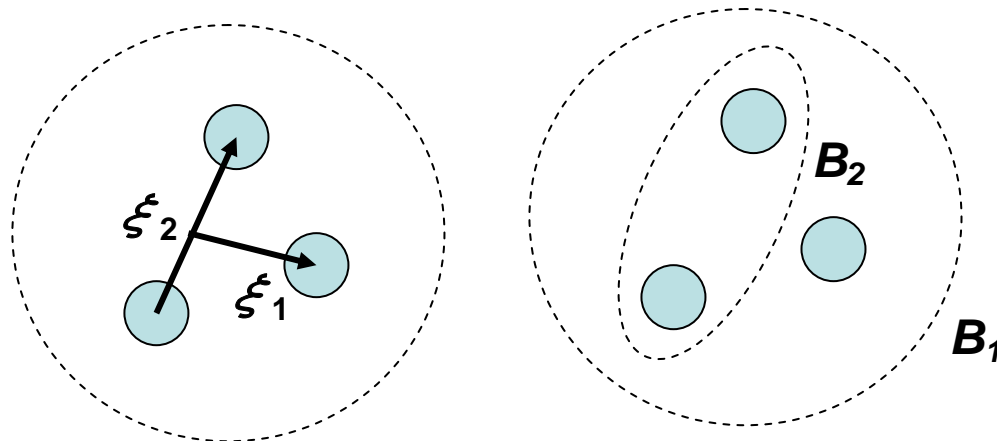
**Non-localized cluster dynamics gives rise to molecular structure in two-cluster systems.**

In relatively simple systems, one kind of size parameter is enough.

But, in relatively complex systems, we will need more than one kind of size parameters:



Effective separation between clusters due to Pauli repulsion



One way is to associate, for each Jacobi coordinate  $\xi_i$ , a GC parameter  $B_i$ .

# Conclusion

**Container picture gives a unified description of cluster-gas states, nuclear molecular states and shell-model-like states.**

**Important dynamical quantity is size-parameter of the system instead of complex coupling of inter-cluster relative motions.**

**In the container picture, inter-cluster Pauli principle is another important ingredient which gives rise to the effective localization of clusters in two-cluster systems.**

**The container of the container picture implies mean field of clusters governed by size parameter of the system.**